Original

Estimation of the Time of Cesium Leaking by Moisture Absorption of Radiologically Contaminated Municipal Solid Waste Incinerator Fly Ash

Tsuneki ICHIKAWA[1, 2*], Kazuo YAMADA[2], and Masahiro OSAKO[2]

[1]Hokkaido University (Home address: 8-1-27 Tonden 3, Kita-ku, Sapporo, Hokkaido 002-0853, Japan)
[2]National Institute for Environmental Studies (16-2 Onogawa, Tsukuba, Ibaraki 305-8506, Japan)

Summary

For estimating the time of cesium leaking from municipal solid waste incinerator fly ash (MSWI FA) containing deliquescent salts and radioactive cesium that had been released by Fukushima Daiichi Nuclear Accident, the rate of moisture absorption of MSWI FA from the atmosphere was measured by changing temperature, relative humidity, bulk density, the contents of $CaCl_2$, NaCl, KCl and pre-absorbed water, and the shape and the structure of the container. The experimental results were summarized with simple mathematical equations which enable one to determine the time period for the leaking from MSWI FA stored in a container under varying temperature and humidity. It was found that the leaking starts when all the pores in the FA are filled with an aqueous solution generated by the moisture absorption, and the time of the leakage is possible to be estimated by solving a simple diffusion equation. The estimated time was more than 11 years for one cubic meter of MSWI FA stored in an air-permeable flexible container under the field condition near Fukushima Daiichi nuclear power plants.

1. Introduction

The Fukushima Daiichi nuclear accident induced by the East Japan earthquake and tsunami of March 11, 2011 released approximately 1.8×10^{16} Bq of ^{134}Cs and 1.5×10^{16} Bq of ^{137}Cs[1-4], which contaminated plants, soils, houses and so on around the reactor site. The demolished houses, plants and other wastes were collected in incineration facilities as municipal solid wastes, and incinerated for volume reduction. Since Cs in the wastes was volatile at high temperature, most of radioactive Cs was concentrated in the municipal solid waste incinerator fly ash (MSWI FA). More than 100,000 tons of radioactive Cs-contaminated MSWI FA is now accumulated in Japan[5, 6]. Most of them are stored in cylindrical flexible containers (Flecon bags) of about 110 cm diameter and 100 cm height made of thick woven polypropylene either coated or uncoated. Although their radioactivity has been significantly reduced by the natural decay of ^{134}Cs (half-life $\approx$ 2 years), a part of the MSWI FA still maintains the radioactivity higher than

8,000 Bq/kg, which prevents the disposal of the MSWI FA as non-radiative waste[5, 6].

MSWI FA is composed of water-insoluble fine particles and water-soluble inorganic salts. The main component of radioactive Cs in MSWI FA is water-soluble CsCl[7-9]. To preventing the radioactive contamination of the storage sites, it is necessary to prevent the penetration of water during its long storage time comparable to the lifetime of ^{137}Cs (half-life $\approx$ 30 years)[10]. Although the MSWI FA is generally stored in facilities that prevent the direct penetration of liquid water such as rainfall and runoff water, water can still penetrate into the MSWI FA by the condensation of water vapor by a temperature difference and moisture absorption of the MSWI FA. MSWI FA contains a significant amount of CaClOH and/or $CaCl_2$ that are generated by the reaction of HCl in the flue gas and $Ca(OH)_2$ added for neutralizing the flue gas[11-13]. Since $CaCl_2$ is a hygroscopic and deliquescent substance that is widely used as a desiccant, and CaClOH reacts with water

*Corresponding author : E-mail: tsuneki@eng.hokudai.ac.jp

to generate $CaCl_2$ and $Ca(OH)_2$ at ambient temperature[14], MSWI FA exposed to humid air is possible to absorb enough amount of water for inducing the leaking of radioactive Cs[15, 16]. To estimate the time of Cs leaking by the moisture absorption is therefore important for certifying the safety of the storage facilities of radiologically contaminated MSWI FA. However, as far as the authors know, no study has been carried out on the moisture absorption of MSWI FA.

In the present paper, the rate of moisture absorption of MSWI FA was measured as functions of temperature, relative humidity, the composition of the FA, and the air-permeability of the container. It was found that the leaking started when the volume of the resultant solution exceeds 1.7 times the volume of water-insoluble particles in the FA, and the time of the leaking is possible to be estimated by solving a simple diffusion equation. Although this study was carried out for the safe storage of radioactive MSWI FA, the obtained results may also be useful for preventing the leakage of the other water-soluble hazardous materials from MSWI FA stored under a humid condition.

2. Materials and Methods

Two types of MSWI FA were used for the experiments. One was MSWI FA as received from stoker-fired and fluidized-bed incinerator plants. The other was artificial MSWI FA that was prepared by adding $CaCl_2$, NaCl and KCl to washed MSWI FA, then drying the mixture for overnight at 230ºC, and finally crushing into fine grains with a crusher (WONDER CRUSHER WC-3, Osaka Chemical Co., Ltd.). Water was added to the crushed MSWI FA, if necessary. MSWI FA was packed into 100 mL, 200 mL or 300 mL measuring cylinders of the cross section of 13.4 cm², or in cylinders of the height of 10 cm and the cross section of 46.6 cm² with an air-tight side wall or an air-penetrable side wall composed of a standard Flecon sheet of the breathability of 55 g/m²·h and the air permeability of 3.5 cm³/cm²·s. Unless otherwise stated, the moisture absorption rate was measured by packing 200 mL of MSWI FA into a 200 mL measuring cylinder. The bulk density of MSWI FA in a cylinder was adjusted by tapping the cylinder. Cylinders with MSWI FA were put into a constant temperature humidity chamber (Yamato, IG400). The total amount of absorbed water was determined by measuring the weight gain of the FA. The concentration of water in the FA was determined by measuring the weight loss of the FA after drying for overnight at 230ºC.

The maximum amount of water absorbed by a substance under given temperature and humidity (moisture absorption capacity) of the mixed salts of $CaCl_2$, NaCl and KCl was determined by measuring the weight of the wet salts in equilibrium with given temperature and relative humidity.

The elemental analysis of MSWI FA was carried out by using an X-ray fluorescence spectrometer (RIX-3100, Rigaku Corporation). The contents of water-soluble components in MSWI FA were determined by using an inductively coupled plasma optical emission spectrometer (Vista-Pro, Varian Inc.). The washing solutions for the analysis were obtained by adding 400% by mass (wt%) of water to MSWI FA, shaking the mixture for overnight, and then filtrating it through 0.45 micron membrane filters. The volume of water-insoluble residues was measured by immersing them in water in a measuring cylinder.

3. Results and discussion

(1) Mechanism of moisture absorption and Cs leaking

Shown in Table 1 are examples of the main constituents

Table 1   **Main components in MSWI FA from stoker-fired and fluidized-bed incinerators**

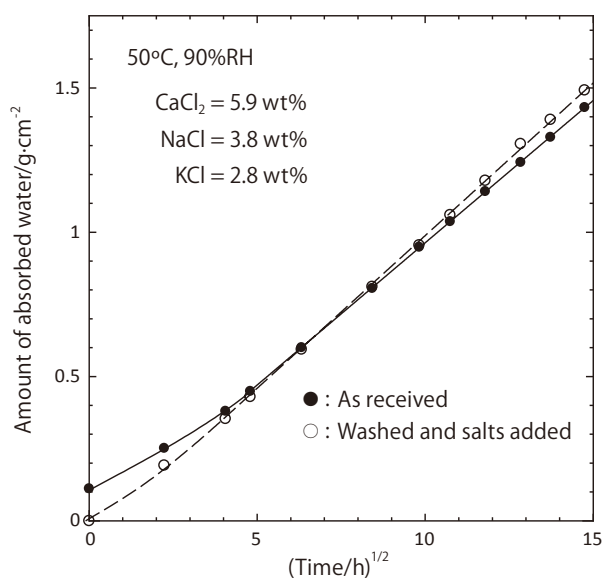| Element	Stoker-fired MSWI FA	Fluidized-bed MSWI FA
Ca	23.3 wt% (23.6 wt% as $CaCl_2$)	21.3 wt% (5.9 wt% as $CaCl_2$)
Na	3.2 wt% (5.8 wt% as NaCl)	4.1 wt% (3.8 wt% as NaCl)
K	4.0 wt% (6.8 wt% as KCl)	3.1 wt% (2.8 wt% as KCl)
Cs	2.7 ppm (2.2 ppm as CsCl)	1.8 ppm (1.4 ppm as CsCl)
Cl	25.2 wt%	10.2 wt%
Mg	0.6 wt%	1.8 wt%
Al	2.3 wt%	5.5 wt%
Si	7.7 wt%	8.3 wt%
P	0.2 wt%	1.0 wt%
S	2.1 wt%	1.0 wt%
Ti	0.3 wt%	1.0 wt%
Fe	0.7 wt%	2.1 wt%
Zn	0.8 wt%	0.6 wt %

Fig. 1 Moisture absorption of original MSWI FA (solid circles) and artificial MSWI FA (open circles) containing the same amounts of $CaCl_2$, NaCl and KCl as those of the original one

Fig. 2 Effect of bulk density and cross section on the moisture absorption of MSWI FA

of MSWI FA obtained from Stoker-fired and fluidized-bed incinerators. MSWI FA generally contains three kinds of hygroscopic salts, $CaCl_2$, NaCl and KCl. These salts constituted more than 99 wt% of total water-soluble constituents. It is noted that CaClOH in dry MSWI FA was measured as $CaCl_2$ in the washing solution.

For elucidating the mechanism of moisture absorption and Cs leaking, it was necessary to control the concentration of the hygroscopic salts in MSWI FA. Fluidized-bed MSWI FA in Table 1 was therefore washed with water to eliminate water-soluble compounds and then $CaCl_2$ was added to the washed FA. NaCl and KCl were further added, if necessary. Fig. 1 compares the moisture absorption rates of the original FA and an artificial FA that was prepared by adding the same amounts of $CaCl_2$, NaCl and KCl as those of the original FA to the washed FA. The similarity of the moisture absorption profiles indicates that artificial MSWI FA was possible to be used for elucidating the moisture absorption and leaking mechanisms of real MSWI FA. The amount of absorbed water linearly increased with the square root of absorption time except for the initial stage of the moisture absorption, which suggests that the rate determining process of moisture absorption was a diffusion process.

Although the bulk density of MSWI FA was difficult to be controlled precisely, as shown in Fig. 2, the moisture absorption rate was not so sensitive to the variation of the bulk density. The decrease of the diffusion rate of moisture by the increase of the bulk density might be compensated
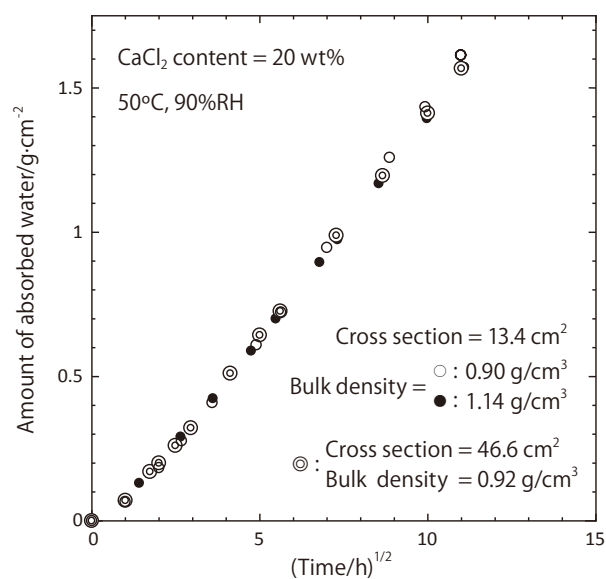
by the increase of the concentration of $CaCl_2$ inducing the increase of the moisture absorption rate. As also shown in Fig. 2, the cross section of MSWI FA did not affect the moisture absorption rate as long as the amount of the absorbed water was normalized with the cross section.

For elucidating the long-term moisture absorption process of MSWI FA leading to the leaking of Cs, MSWI FA containing 10 wt%, 20 wt% and 30 wt% of $CaCl_2$ were packed in nine measuring cylinders to the volumes of 100 mL, 200 mL and 300 mL with the bulk densities of 0.90~0.92, and exposed to air with 90 %RH under the accelerated condition at 50ºC. It is noted that the moisture absorption capacity of unit amount of dry $CaCl_2$ under a given relative humidity scarcely depends on the temperature[15, 16], since the activation energy for water evaporation is approximately the same for water and the solution. Fig. 3 shows the amount of absorbed water as a function of the moisture absorption time. The amount of absorbed water did not depend on the amount of the FA and linearly increased with the square root of the time of moisture absorption. As shown in Fig. 4, the absorption of water caused the development of dark wetting bands, though the total volumes of the FA were kept constant. The depth of the wetting front also increased with the square root of the time of moisture absorption (Fig. 5). Although both the amount of absorbed water and the progress of the wetting band followed the square root of the time, which generally implies that the rate determining processes are a diffusion
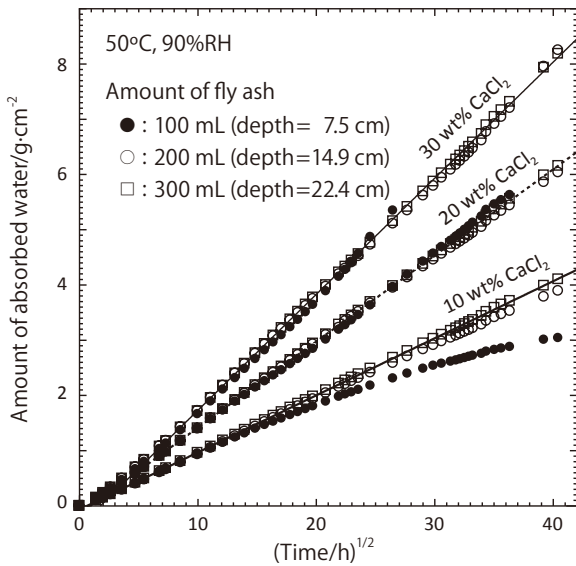
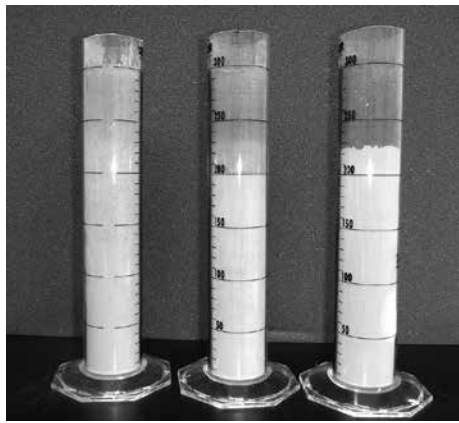**Fig. 3** Time evolution of the amount of absorbed water in MSWI FA

Fig. 4 **Wetting bands developed during moisture absorption of MSWI FA in the atmosphere at 50ºC and 90 %RH**
The contents of CaCl₂ are, from left to right, 10 wt%, 20 wt% and 30 wt%, respectively.
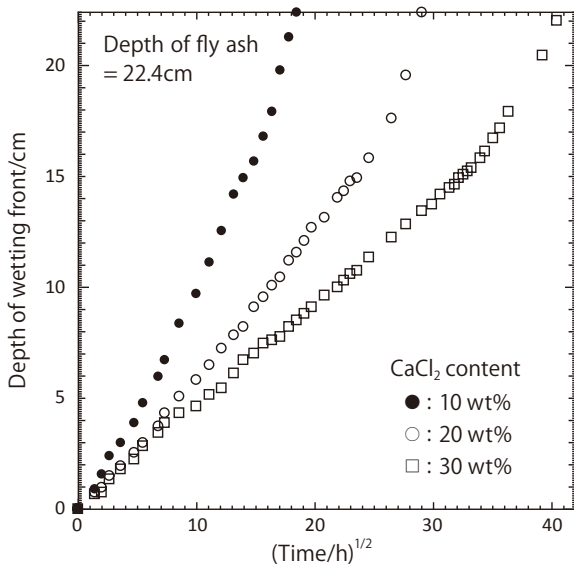

Fig. 5 Time evolution of the location of wetting front in 300 mL MSWI FA

process, the rate determining process of moisture absorption was not the diffusion of water vapor from the surface to the wetting front where the moisture was condensed, because the amount of absorbed water increased with the square root of time even after reaching of the wetting front to the bottom of the cylinder.

Fig. 6 shows the wetting condition of MSWI FA in 100 mL cylinders after moisture absorption for 1100 hours. The leaking of the $CaCl_2$ solutions (and Cs, if unwashed) from the FA took place in 100 mL cylinders at 1000 hours and 600 hours for the 20 wt% and 30 wt% $CaCl_2$ samples, respectively, after starting the moisture absorption. The volumes of the samples were kept constant before the leaking, so that the leaking was started when the resultant solution completely filled the space in MSWI FA which were initially filled with air and water-soluble $CaCl_2$. Table 2 compares the total volume of the space and the volume of the $CaCl_2$ solution when the leaking started. The volume of the space is very close to the volume of the $CaCl_2$ solution, which confirms that the leaking took place when the solution filled the space between water-insoluble particles. The leaking did not take place for the 10 wt% $CaCl_2$ sample because the maximum amount of absorbed water was not enough for filling the pores even at 90%RH.

Fig. 7 shows the depth profiles of the contents of water and $CaCl_2$ for 30 wt% $CaCl_2$ samples in 200 mL and 300 mL cylinders after the moisture absorption for 2000 hours. Although the spatial distribution of $CaCl_2$ had been uniform before the moisture absorption, the content of $CaCl_2$ after the absorption increased with increasing the depth. This increase suggests that a part of the $CaCl_2$ solution migrated to the bottom due to capillary suction of pores in the FA.
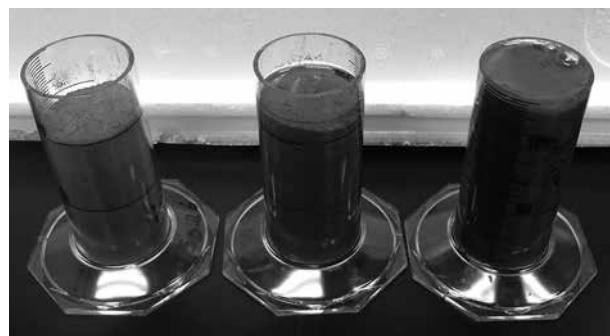

Fig. 6. **Wetting conditions of 100 mL MSWI FA after moisture absorption for 1100 hours in the atmosphere at 50ºC and 90%RH**
The contents of CaCl₂ are, from left to right, 10 wt%, 20 wt% and 30 wt%, respectively.

Table 2   **Pore volume and the volume of CaCl₂ solution when the leaking of CaCl₂ solution from 100 mL of MSWI FA started**

CaCl₂ content	Water content	CaCl₂ solution volume[a]	Pore volume
20 wt% (0.18 g/cm³)	65 g	69 cm³	68 cm³
30 wt% (0. 27g/cm³)	72 g	78 cm³	72 cm³

[a] The volume of the solution was estimated from the weight and the density of CaCl₂ solution[17].
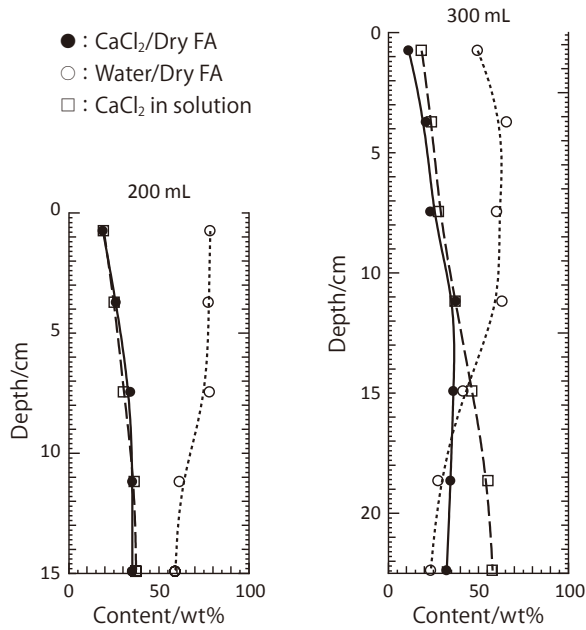

Fig. 7   **Depth profiles of the contents of water and CaCl₂ for MSW FA containing 30 wt% of CaCl₂ in 200 mL and 300 mL cylinders after 2000 hours moisture absorption at 50ºC 90%RH**

The concentration of CaCl₂ in the aqueous solution near the surface of the samples, 15 wt%, was very close to the equilibrium concentration under 90 %RH. The concentration monotonously increased with increasing th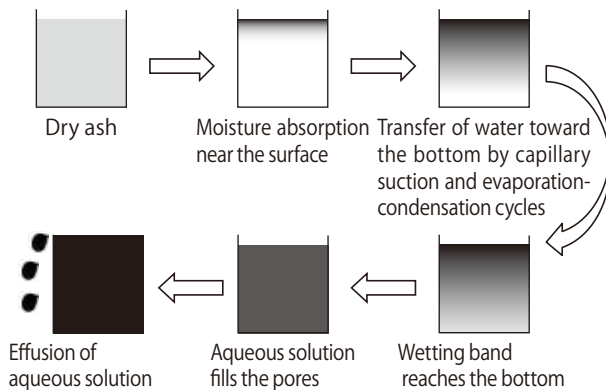e depth. These results indicate that moisture was absorbed near the surface of MSWI FA and then transferred to the inner part by repeated evaporation-condensation cycles and capillary suction. The gravitational force did not affect the migration of the CaCl₂ solution toward the bottom, because the moisture absorption rate was the same even the cylinder was tilted by 90 degrees. The depth profiles for 20 wt% CaCl₂ samples were essentially the same as those for the 30 wt% samples. The mechanism of Cs leaking by moisture absorption is schematically depicted in Fig. 8.

Although the volume of MSWI FA in 100 mL cylinders was kept constant until the leaking started, due to self-weight consolidation, the volume of MSWI FA in a flexible container of 1 m³ may decrease with increasing the amount of absorbed water. Fig. 9 shows the volume change of washed MSWI FA slurry after packing in a plastic cylinder with an inner diameter of 5 cm to a height of 99 cm. The excess water generated by the sedimentation of the slurry was initially removed from the top of the cylinder by aspiration. The true volume of the washed FA was 681 cm³. The excess water resulting from the consolidation was continuously removed from the bottom of the cylinder through a stainless 100 mesh screen. Due to the consolidation, the apparent
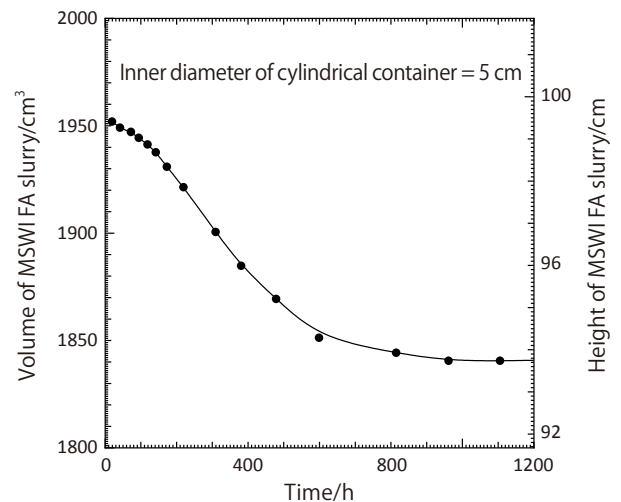

Fig. 8   Mechanism of Cs leaking from MSWI FA by moisture absorption

Fig. 9   Self-weight consolidation of washed MSWI FA slurry in a cylindrical container

volume of the FA was slowly decreased from the initial value of 1950 cm³ to the final value of 1840 cm³. Since 1840 cm³ of the wet FA was composed of 681 cm³ of water-insoluble particles and 1159 cm³ of water, it is concluded that 1 cm³ of water-insoluble particles in MSWI FA can hold 1.7 cm³ of liquid without leaking. The liquid-holding capacity of the FA, the volume fraction of liquid that can be held by the FA without leaking, is then estimated as

$$w_{max} = 1.7 / (1 + 1.7) \equiv 0.63 \quad \cdots \cdots \cdots \cdots \cdots \cdots \cdots \quad (1)$$

The degree of the consolidation generally increases with increasing the height of stored FA. However, since the height of stored MSWI FA is generally less than 100 cm, it is safe enough to assume that the Cs leaking by moisture absorption does not take place until the volume of liquid reaches 1.7 times the volume of the water-insoluble particles in MSWI FA. The volume of salts solutions are not much different from the volume of water in the solutions, so that w_{max} can be regarded as the maximum amount of water that can be absorbed by unit volume of MSWI FA without Cs leaking.

(2) Moisture absorption under various temperature and humidity

For estimating the time of Cs leaking from stored MSWI FA, the rates of moisture absorption by MSWI FA in 200 mL cylinders containing 10 wt%, 20 wt% and 30 wt% of CaCl₂ were measured at the temperatures of 10°C, 20°C, 30°C and 40°C and the humidities of 50%RH, 70
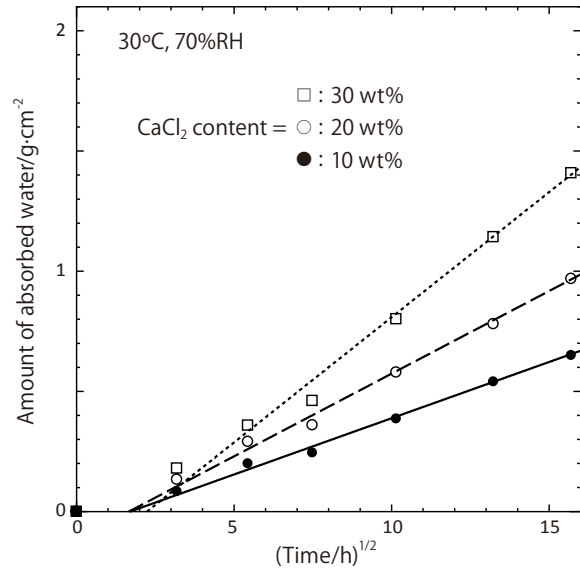

Fig. 10 **Effect of the content of CaCl₂ on the moisture absorption of MSWI FA at 30°C and 70%RH**

%RH and 90%RH. Fig. 10 shows examples of the moisture absorption. Except for very early stage of the moisture absorption, the amount of absorbed water per unit cross section, W, followed the square root of time law, as

$$W = (kt)^{1/2} \quad \cdots \cdots \cdots \cdots \cdots \cdots \cdots \cdots \cdots \cdots \cdots \cdots \cdots \quad (2)$$

where k is the rate constant of moisture absorption, and is a function of temperature, humidity and the intrinsic nature of MSWI FA such as the content of CaCl₂. Table 3 summarizes the values of observed k in g²/cm⁴·h unit.

Table 3 **Comparison of the observed rate constants of moisture absorption (g²/cm⁴h) with calculated ones obtained by using Eq. (2)[a]**

CaCl₂ content	10 wt%		20 wt%		30 wt%	
Condition	Observed	Calculated	Observed	Calculated	Observed	Calculated
10°C 50%RH	0.00028	0.00022	0.00048	0.00054	0.00108	0.00109
10°C 70%RH	0.00067	0.00070	0.00164	0.00168	0.00374	0.00343
10°C 90%RH	0.00143	0.00016	0.00356	0.00396	0.00865	0.00806
20°C 50%RH	0.00044	0.00040	0.00096	0.00097	0.00196	0.00197
20°C 70%RH	0.00110	0.00126	0.00270	0.00303	0.00613	0.00618
20°C 90%RH	0.00303	0.00296	0.00951	0.00712	0.01788	0.01452
30°C 50%RH	0.00075	0.00069	0.00181	0.00167	0.00326	0.00341
30°C 70%RH	0.00219	0.00218	0.00473	0.00525	0.01084	0.01070
30°C 90%RH	0.00554	0.00512	0.01400	0.01233	0.02460	0.02514
40°C 50%RH	0.00145	0.00116	0.00297	0.00279	0.00538	0.00570
40°C 70%RH	0.00334	0.00364	0.00820	0.00877	0.01463	0.01789
40°C 90%RH	0.00834	0.00856	0.02226	0.02062	0.04284	0.04204

[a] Eq. (2): $k = A_0 RH^{3.4} \exp(-4880/T)$, where A_0 in g²/cm⁴h unit is 0.0114 for 10 wt% CaCl₂, 0.0274 for 20 wt% CaCl₂, and 0.0559 for 30 wt% CaCl₂ samples, RH is relative humidity in % unit, and T is absolute temperature.
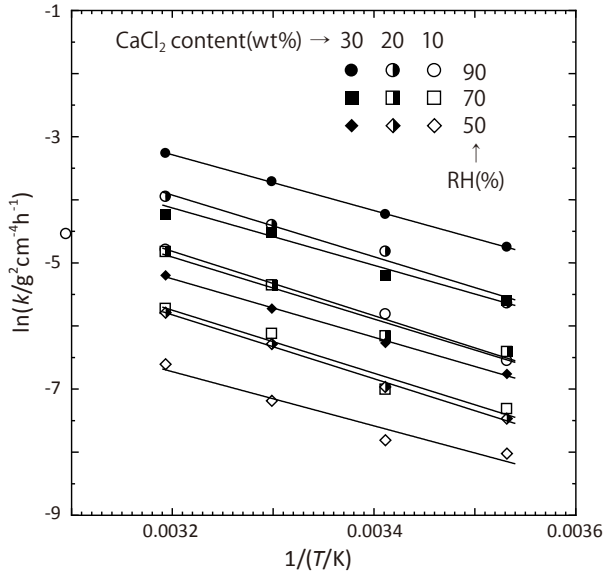
Fig. 11 **Arrhenius plots of the rate constant k of moisture absorption**
The relative humidity and the content of CaCl$_2$ for each k are shown with a low and column matrix. Solid lines show the best fits for the observed rate constants.

Fig. 11 shows the Arrhenius plots of k for the same humidity and CaCl$_2$ content groups against absolute temperature T. The activation energy terms determined from the slopes of the best fit lines ranged between -5101 and -4301. These values are close to the activation energy term of -5280 for the evaporation of pure water, which suggests that the rate determining process of moisture absorption was the migration of water vapor from the moisture-saturated CaCl$_2$ solution near the surface of MSWI FA to the inner part where the CaCl$_2$ solution was not saturated with moisture. The unsaturated solution near the surface then absorbed moisture until reaching the equilibrium concentration. A single activation energy term minimizing the difference between the observed and estimated rate constants was -4880, so that -4880 was adopted as the activation energy term irrespective of the humidity and the content of CaCl$_2$.

Fig. 12 shows the humidity dependency of the rate constants. The log-log plots of relative humidity vs temperature-corrected rate constants for the same CaCl$_2$ content groups give straight lines with the slope of approximately 3.4. The rate constants are therefore approximately expressed by equation

$$k = A_0 RH^{3.4} \exp(-4880/T) \quad \cdots\cdots\cdots\cdots (3)$$

where A_0 is a constant in g^2/cm^{4}h unit with a value depending on the intrinsic nature of MSWI FA such as the concentration

of CaCl$_2$, RH is relative humidity in %unit, and T is absolute temperature. The best values of A_0 were 0.0114 for 10 wt% CaCl$_2$, 0.0274 for 20 wt% CaCl$_2$, and 0.0559 for 30 wt% CaCl$_2$ samples. The rate constants thus derived are also shown in Table 3. They are in good agreement with the observed ones within the variance of 0.031.

(3) Moisture absorption under fluctuating temperature and humidity

Since the temperature and the humidity of air surrounding MSWI FA are usually fluctuated, for correct estimation of the time of the leaking, it is necessary to elucidate the effect of the fluctuations on the moisture absorption rate. Fig. 13 shows the moisture absorption profile of a 20 wt% CaCl$_2$ sample under stepwise change of the temperature of 20°C and 30°C and the humidity of 70%RH and 90%RH. Decrease of the humidity caused the decrease of the amount of absorbed water by evaporation, which certifies that the concentration of the CaCl$_2$ solution near the surface of the sample was in equilibrium with the atmospheric humidity. After reaching the equilibrium concentration, the solution re-started to absorb moisture and transferred the water toward the bottom by evaporation and capillary suction. The amount of water therefore increased again. The decrease of water content did not take place when only the temperature was changed, since the equilibrium concentration did not depend on the temperature. When the humidity was increased, the concentration of CaCl$_2$ near the surface became higher than the equilibrium
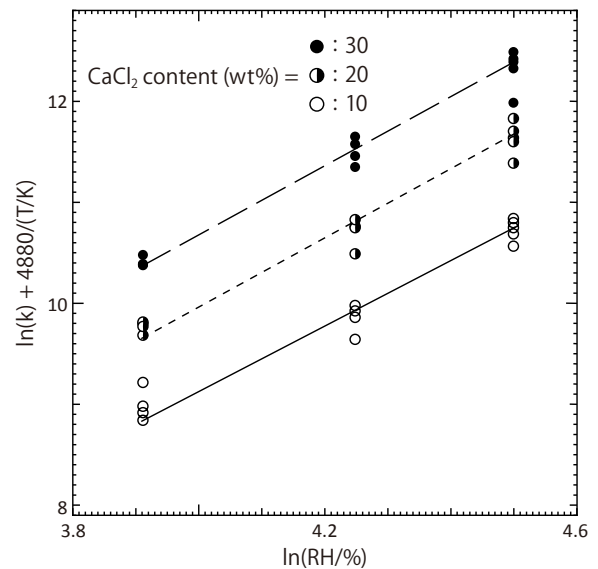

Fig. 12 **Effects of relative humidity and CaCl$_2$ content on the rate constant k of moisture absorption**

concentration. The rate of moisture absorption therefore became higher than that predicted by the square root of time law. After reaching the equilibrium concentration, the absorption rate followed the square root of time law again. When only the temperature was changed, the square root of time law was maintained but the slope of the line was changed.

Since the decrease and the increase of the humidity caused the deceleration and the acceleration of the moisture absorption, it is expected that these fluctuations are averaged out during long period of moisture absorption. The amount of absorbed water at time t, $W(t)$, is then approximately given by neglecting the deceleration and the acceleration processes as

$$W(t) = \left[\int_0^t k(t)dt \right]^{1/2} = \left[\int_0^t A_0 [RH(t)]^{3.4} \exp[-4880 / T(t)]dt \right]^{1/2} \cdots\cdots\cdots\cdots (4)$$

where $k(t)$, $RH(t)$ and $T(t)$ are the rate constant, relative humidity and absolute temperature at time t, respectively. As shown in Fig. 13 with a solid curve, except for the deceleration and the acceleration periods, the observed amount of absorbed water compares well with that calculated with Eq. (4).

Fig. 14 shows the response of moisture absorption upon short-period temperature and humidity fluctuation of the repeated cycles of "keeping 40ºC 80%RH for 6

hours → linear decrease of the temperature and humidity toward 25 ºC 60 %RH for 6 hours → keeping 25ºC 60 %RH for 6 hours → linear increase of the temperature and humidity toward 40 ºC 80 %RH for 6 hours". The moisture absorption initially followed the square root of time law with a single rate constant. The rate constant was very close to the average rate constant of $k_{av} = 0.00739$ that was derived from equations

$$RT_{av} = \frac{1}{t_c} \int_0^{t_c} [RH(t)]^{3.4} \exp[-4880 / T(t)]dt \quad \cdots\cdots\cdots (5)$$

$$k_{av} = A_0 RT_{av} \quad \cdots\cdots\cdots\cdots\cdots\cdots\cdots\cdots\cdots\cdots\cdots (6)$$

where t_c is the time of one cycle and is 24 hours in the present case, and $A_0 = 0.0274$ for 20 wt% CaCl$_2$ samples. After 300 hours, the moisture absorption rate gradually slowed down toward the maximum amount of 27 g. The maximum amount was very close to the equilibrium amount of moisture absorption (28 g) at the weight-average humidity of $RH_{av} = 75$ %RH that was derived from the following equation.

$$RH_{av} = \frac{1}{RT_{av}t_c} \int_0^{t_c} RH(t)[RH(t)]^{3.4} \exp[-4880 / T(t)]dt \quad \cdots (7)$$

These results indicate that the fluctuation of humidity and temperature is averaged out to give single rate constant, humidity and temperature defined by Eqs. (5), (6), (7) and

$$T_{av} = \frac{1}{RT_{av}t_c} \int_0^{t_c} T(t)[RH(t)]^{3.4} \exp[-4880 / T(t)]dt \quad \cdots\cdots\cdots (8)$$
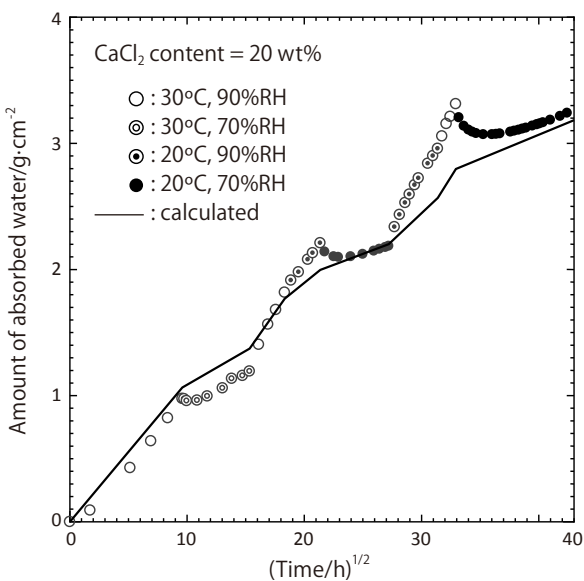

Fig. 13 Moisture absorption profile of MSWI FA under stepwise change of the temperature of 20ºC and 30ºC and the humidity of 70%RH and 90%RH
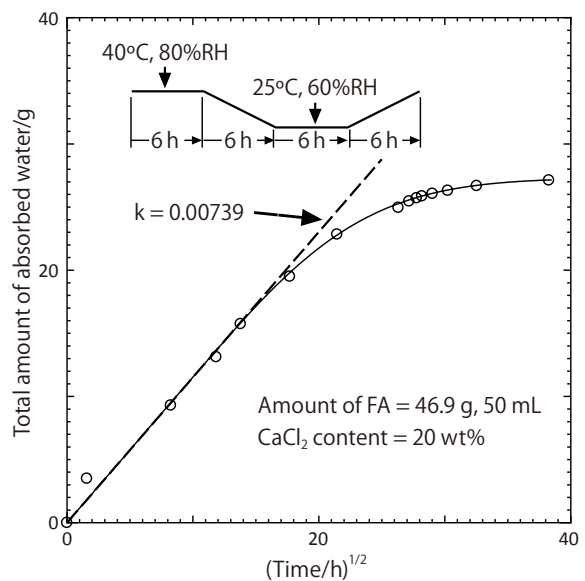

Fig. 14 Moisture absorption profile of MSWI FA under repeated temperature and humidity fluctuation cycles

(4) Effect of NaCl, KCl and pre-absorbed water

Although NaCl and KCl alone are hygroscopic only above 75 %RH and 84 %RH, respectively, once they are dissolved in a $CaCl_2$ solution, they can absorb moisture even below their critical humidity. Since no data had been available on the equilibrium humidity for the ternary solution system, the moisture absorption capacity of the mixture of $CaCl_2$, NaCl and KCl was measured as a function of relative humidity. Table 4 shows the moisture absorption capacity of the mixed solids of $CaCl_2$, NaCl and KCl as a function of relative humidity and temperature. Due to the dissolution of NaCl and KCl, the moisture absorption capacity of the mixture was higher than that of pure $CaCl_2$ even at 50 %RH. Although the moisture absorption capacities of individual salts scarcely depend on the temperature, due to temperature dependency of the solubility of NaCl and KCl in the $CaCl_2$ solution, the moisture absorption capacity of the mixture was slightly temperature dependent.

The effect of coexisting NaCl and KCl on the time of Cs leaking was evaluated by assuming that 1 g of NaCl and KCl correspond to a g and b g of $CaCl_2$, respectively, where the values of a and b were humidity-dependent. The moisture absorption capacity v of the solid mixture containing 1 g of $CaCl_2$, x g of NaCl and y g of KCl was then estimated by equation

$$v = (1 + ax + by)v_{eq} \quad \cdots\cdots\cdots\cdots\cdots\cdots\cdots\cdots \quad (9)$$

where v_{eq} is the moisture absorption capacity of 1 g of pure $CaCl_2$ under given hymidity. The values of conversion factors a and b under given relative humidity were determined in such a way to minimize the difference between the observed and estimated moisture absorption capacities. As shown in Fig. 15, the estimated values compared well with the observed ones. The values of a and b at 70 %RH, typical average annual humidity in Japan, are 0.85 and 0.45, respectively.

For preventing the scattering of MSWI FA, the FA has occasionally been stored after adding 20 wt% to 30 wt% of water. Fig. 16 shows the effect of pre-absorbed water on the moisture absorption of MSWI FA containing 20 wt% and 30 wt% of $CaCl_2$. Although the moisture absorption was slightly suppressed by the pre-absorbed water which was homogeneously distributed in the FA, the square root of time law was still maintained except for the early stage of moisture absorption.

Since the effects of humidity and temperature on moisture absorption had been examined only on artificially pre-

Table 4   Moisture absorption capacity of the mixed solids of CaCl₂, NaCl and KCl under different humidity and temperature

| Feed			Amount of absorbed H₂O/g at different temperature and relative humidity					
CaCl₂/g	NaCl/g	KCl/g	25°C, 50%RH	25°C, 60%RH	25°C, 70%RH	15°C, 70%RH	25°C, 80%RH	25°C, 90%RH
1.00	0.00	0.00	1.79	2.09	2.62	2.65	3.46	5.59
1.00	0.20	0.00	1.84	2.32	3.20	3.23	4.30	6.46
1.00	0.40	0.00	1.88	2.32	3.66	3.47	4.80	7.58
1.00	0.70	0.00	1.84	2.30	3.96	3.47	5.64	8.96
1.00	0.00	0.20	1.80	2.26	2.94	2.81	3.72	5.78
1.00	0.20	0.20	1.91	2.48	3.30	3.23	4.31	6.44
1.00	0.40	0.20	1.88	2.52	3.82	3.59	5.04	7.52
1.00	0.69	0.20	1.87	2.50	4.33	4.02	5.93	9.26
1.00	0.00	0.40	1.88	2.26	3.06	2.97	4.22	6.20
1.00	0.20	0.40	1.88	2.52	3.64	3.37	4.88	7.18
1.00	0.40	0.40	1.88	2.46	4.06	3.85	5.62	9.10
1.00	0.70	0.40	1.87	2.48	4.69	4.48	6.60	10.48
1.00	0.00	0.70	1.84	2.24	3.06	2.99	4.86	7.42
1.00	0.20	0.70	1.90	2.50	3.86	3.59	5.48	8.72
1.00	0.40	0.72	1.86	2.56	4.26	4.01	6.14	10.30
1.00	0.70	0.70	1.90	2.48	4.92	4.53	6.90	10.82
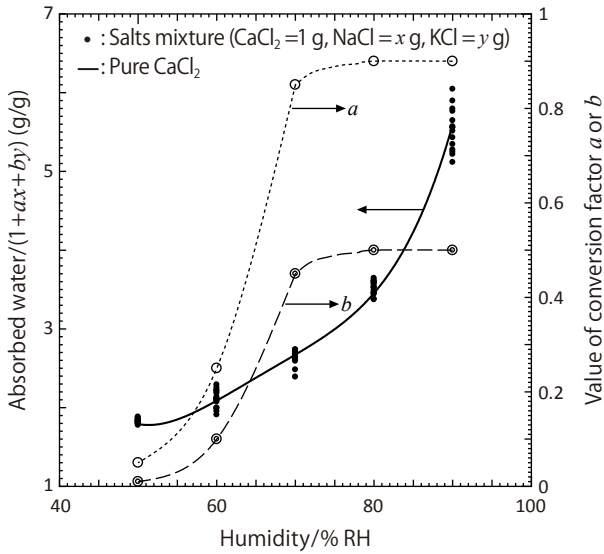
Fig. 15 Comparison of observed moisture absorption capacities of the mixtures of CaCl$_2$, NaCl and KCl (solid circles) with those derived from Eq. (6) (solid curve)

Fig. 16 Effect of pre-absorbed water on moisture absorption

pared MSWI FA, the effects were examined on as-received unwashed MSWI FA. Fig. 17 shows the rate of moisture absorption of MSWI FA containing 16.1 wt% of CaCl$_2$, 3.6 wt% of NaCl, 8.8 wt% of KCl and 21.1 wt% of water. The moisture absorption also followed the square root time law. The rate constant of moisture absorption at 30℃ and 70 % RH was $(70/90)^{3.4}$ times slower than that at 30℃ and 90 % RH. Fig. 18 shows the Arrhenius plot of the rate constants at 90 % RH as a function of absolute temperature. The value of the activation term is -4880, in accordance with that without NaCl and KCl. These evidences suggest that Eq. (3) is applicable for MSWI fly ash containing CaCl$_2$, NaCl, KCl and water. The values of a and b are strongly humidity-dependent below 70 % RH, so that it is questionable whether the relation of $RH^{3.4}$ is maintained below 70 %RH. However, the error arising from the fluctuation of a and b can be minimized by using the values at average annual humidity.

(5) Effect of air-permeable side wall

So far we have treated the moisture absorption of MSWI FA in a cylinder composed of an air-tight side wall and a bottom. However a significant amount of MSWI FA is stored in flexible containers made of an air-permeable sheet. Fig. 19 compares the moisture absorption of MSWI FA in cylinders of 7.7 cm diameter (cross section = 46.6 cm^2) with side walls made of an air-tight plastic sheet and an air-permeable standard Flecon sheet of the air permeability of 3.5 cm^3/cm^2・s. Although the real process of moisture
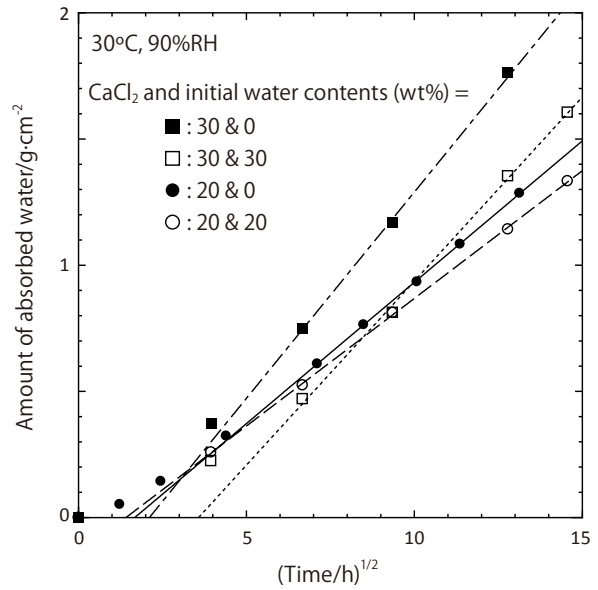
absorption is very complex including condensation-evaporation cycles and capillary suction, after several attempts, we found that the total amount of absorbed water, W_T, was obtained by spatial integration of function P, as

$$W_T = \int P dv \quad \cdots\cdots\cdots\cdots\cdots\cdots\cdots\cdots \quad (10)$$

Here P is a pseudo concentration of absorbed water, and is obtained by solving a simple diffusion equation of

$$\frac{\partial P}{\partial t} = D_w \nabla^2 P \quad \cdots\cdots\cdots\cdots\cdots\cdots\cdots\cdots\cdots \quad (11)$$

where D_w is a pseudo diffusion coefficient and is determined in such a way to reproduce an experimental result. The initial condition for Eq. (11) is

$$P = w_i \quad \cdots\cdots\cdots\cdots\cdots\cdots\cdots\cdots\cdots\cdots \quad (12)$$

where w_i is the initial concentration of absorbed water in weight/volume unit. The boundary conditions for Eq. (11) are

$$\frac{\partial P}{\partial n} = 0 \quad \cdots\cdots\cdots\cdots\cdots\cdots\cdots\cdots\cdots\cdots \quad (13)$$

on an air-tight surface, where n is normal to the surface, and

$$P = w_{eq} \quad \cdots\cdots\cdots\cdots\cdots\cdots\cdots\cdots\cdots\cdots \quad (14)$$

on an air-permeable surface, where w_{eq} in weight/volume unit is the concentration of water that is under equilibrium with the atmosphere.

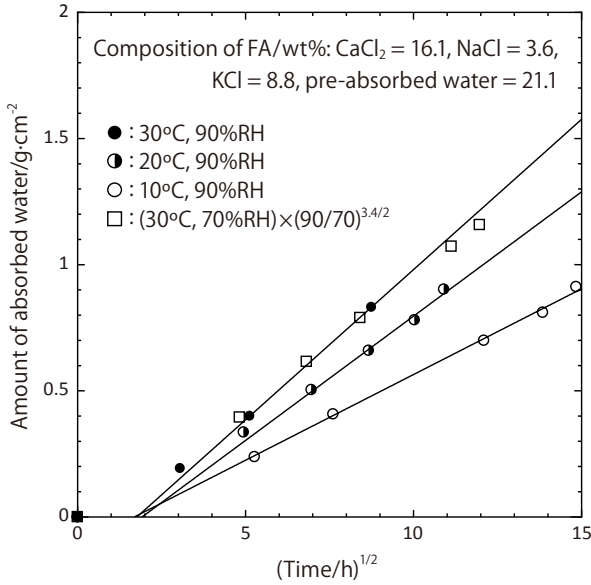The solution of Eq. (10) for a cylindrical sample of

Fig. 17 Moisture absorption of as-received MSWI FA at different temperature and humidity
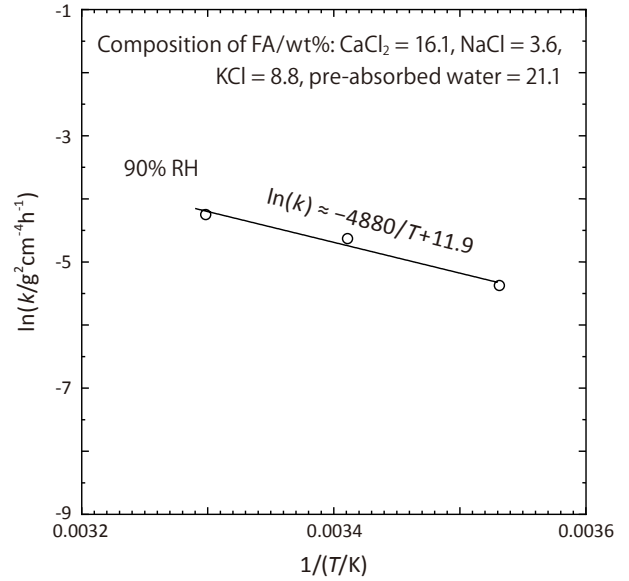

Fig. 18 Arrhenius plot of the rate constant k of moisture absorption for as-received MSWI FA

radius r_0 and height z_0 under moisture absorption from the open top is given by

$$W_T = \pi r_0^2 z_0 \left\{ w_{eq} - (w_{eq} - w_i) \sum_{n=0}^{\infty} \frac{2}{(n+1/2)^2 \pi^2} \exp\left[-(n+1/2)^2 \pi^2 (D_w t / z_0^2) \right] \right\} \cdots\cdots\cdots\cdots (15)$$

The amount of absorbed water per unit area is then given by

$$(W_T - \pi r_0^2 z_0 w_i)/(\pi r_0^2) = z_0 (w_{eq} - w_i) \left\{ 1 - \sum_{n=0}^{\infty} \frac{2}{(n+1/2)^2 \pi^2} \exp\left[-(n+1/2)^2 \pi^2 D_w t / z_0^2 \right] \right\} \cdots\cdots\cdots\cdots (16)$$

Under the condition of $D_w t/z_0^2 \ll 1$, Eq. (16) becomes

$$(W_T - \pi r_0^2 z_0 w_i)/(\pi r_0^2) = \left[4 D_w (w_{eq} - w_i)^2 t / \pi \right]^{1/2} \cdots (17)$$

Comparison of Eq. (2) and Eq. (17) indicates that the pseudo diffusion coefficient D_w is derived from the observed rate constant of moisture absorption, k, as

$$D_w = \frac{\pi k}{4(w_{eq} - w_i)^2} \qquad \cdots\cdots\cdots\cdots\cdots\cdots (18)$$

For a sample in an air-permeable side wall, the moisture absorption rate per unit surface area of the wall is much lower than that of the top surface. The pseud diffusion coefficient for the moisture absorption from the side wall, D_{wF}, is therefore much smaller than D_w. The solution under moisture absorption from the top and the side wall is then given by

$$W_T = \pi r_0^2 z_0 \left\{ w_{eq} - (w_{eq} - w_i) \sum_{n=0}^{\infty} \frac{2 \exp[-(n+1/2)^2 \pi^2 D_w t / z_0^2]}{(n+1/2)^2 \pi^2} \sum_{i=1}^{\infty} \frac{4}{x_i^2} \exp[-(x_i / r_0)^2 D_{wF} t] \right\} \cdots\cdots\cdots\cdots (19)$$

where x_i is the i-th solution of Bessel function $J_0(x) = 0$, and is approximately given by

$$x_i \approx (s_i / 4) \left[\begin{matrix} 1 + 2/s_i^2 - (62/3)/s_i^4 + (15116/15)/s_i^6 \\ -(12554474/105)/s_i^8 + (8368654292/315)/s_i^{10} \end{matrix} \right] \cdots\cdots\cdots\cdots\cdots\cdots\cdots\cdots (20)$$

where $s_i = \pi(4i - 1)$. Best fit of the experimental data gives $D_{wF} = 0.12 D_w$.

Since the real process of moisture absorption is very complex including condensation-evaporation cycles, capillary suction and the change of the effective diffusion

coefficient of moisture due to the change of the porosity of MSWI FA, P itself may not reproduce an observed spatial distribution of water. However, as shown with solid and broken lines in Fig. 19, the total amount of absorbed water reproduces the observed amount quite well.
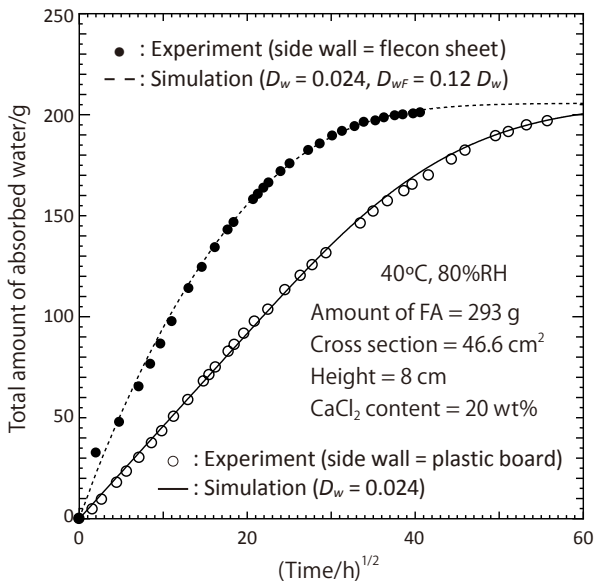
Fig. 19 **Comparison of observed and calculated amounts of moisture absorption of MSWI FA in cylinders with air-tight and air-permeable side walls**

(6) Procedure for estimating the time of Cs leaking

a) Estimation of average annual humidity and temperature

Based on the experimental and mathematical results mentioned so far, in the following section, we descrive the procedure for estimating the time of Cs leaking by using three Stoker-fired MSWI FA samples stored near Fukushima Daiich nuclear plants as an example. Since the rate of moisture absorption and the maximum amount of absorbed moisture are a function of humidity and temperature, for estiming the possibility and the time of the leaking, it is at first necessary to estimate the average annual humidity and temperature by using Eqs. (5), (7) and (8), respecively. Using the annual climate data of Onahama district near Fukushima Daiich Nuclear Plants in 2013 [18], the average humidity and temperature are calculated to be RH_{av} = 83%RH and T_{av} = 292.5 K or 19°C, respectively. They are much higher than the unweighted average values of 72 %RH and 14°C.

b) Evaluation of the possibility of Cs leaking

The possibility of Cs leaking can be evaluated by measuring the moisture absorption capacity w_{eq} of MSWI FA and the volume of water-insoluble particles in the FA in the following manner. The FA is at first dried at 230°C for overnight for measureing the initial content of water. The maximum amount of absorbed water is then determined by keeping the dried FA in a constant temperature humidity chamber at T_{av} = 19°C and RH_{av} =83 %RH until

the weight of the FA becomes constant. Finally, the real volume of water-insoluble particles in the FA is determined after washing the FA. The bulk volume of MSWI FA is assumed to be 2.7 times the true volume of the water-insoluble particles (Eq. (1)), so that w_{eq} is obtained by dividing the weight of the absorbed water with the bulk volume. The values of w_{eq} thus obtained are listed in Table 4 together with the initial content of water w_i. The value of w_{eq} is larger than the liquid-holding capacity of w_{max} = 0.63 for all the samples, so that the leaking of Cs is likely to take place by storing the samples under the field condition.

The possibility of Cs leaking can be numerically evaluated, if the contents of CaCl$_2$, NaCl and KCl in MSWI FA are known. Suppose 1 g of dry MSWI FA contains α g of CaCl$_2$, β g of NaCl and γ g of KCl, the effective content of CaCl$_2$ under the annual average humidity of RH_y becomes (α + $a\beta$ + $b\gamma$), where the values of a and b can be found in Fig. 15. Assuming that the volume of the solution generated by the absorption of the salts is close to the volume of the absorbed water, the volume of the solution generated from 1 g of the FA is given by (α + $a\beta$ + $b\gamma$)v_{eq}, The value of v_{eq} is shown in Fig. 15 with a solid curve. Since 1 cm³ of the insoluble solids can support up to 1.7 cm³ of the solution, Cs will be leaked out if the following relation is fulfilled.

$$(\alpha + a\beta + b\gamma)v_{eq} > 1.7(1 - \alpha - \beta - \gamma)/\rho_S \cdots \cdots (21)$$

Here ρ_s is the density of insoluble solids.

c) Calculation of the time of Cs leaking

Three MSWI FA samples obtained from MSWI facilities in Fukushima prefecture were used for estimating the time for the leaking to start. Table 5 shows the characteristics of the FA. The density of insoluble solids was 2.22 for all the FA. All the FA contained more than 20 wt% of water which had been added for preventing the scattering of the FA. The difference of the moisture absorption capacity w_{eq} at RH_{av} (83%RH) and T_{av} (19°C) reflects the difference of the contents of hygroscopic salts. Fig. 20 shows the rate constants of moisture absorption at RH_{av} and T_{av} for these samples. The value of A_0 necessary for calculating the annual average rate constant is obtained by substituting RH_{av} and T_{av} into Eq. (3). The annual average rate constant is then determined by substituting the values of RT_{av} and A_0 into Eq. (6). The value of RT_{av} defined by Eq (5) has already determined in section (b). The observed and annual average rate constants are also shown in Table 5. The value of pseudo diffusion coefficient D_w is then

Table 5   Parameters used for the estimation of the time of Cs leaking from MSWI FA samples packed in open-top air-tight and air-permeable flexible containers with a diameter of 110cm to the height of 100 cm, and the estimated time

Sample	w_i/g·cm^{-3}	w_{eq}/g·cm^{-3}	k/g^{2}cm^{-4}h^{-1}	k_{av}/g^{2}cm^{-4}h^{-1}	D_w/cm^{2}h^{-1}	Air-tight	Air-permeable
FA1	0.30	1.41	0.0024	0.0016	0.0010	49 years	11 years
FA2	0.24	0.85	0.0019	0.0013	0.0027	92 years	28 years
FA3	0.222	1.03	0.0022	0.0015	0.0018	92 years	26 years

determined by substituting w_i, w_{eq} and the annual average rate constant into Eq. (18), and is shown in Table 5.

Since moisture is penetrated into MSWI FA from the surface that is exposed to the atmosphere, the time of Cs leaking strongly depends on the volume to surface ratio of stored MSWI FA. MSWI FA is usually stored in flexible containers of 110 cm diameter and 110 cm depth to the height of approximately 100 cm. These bags with MSWI FA are generally piled up tightly on a storage area, so that the average volume to surface ratio for the stored MSWI FA is much smaller than that of the container itself. However, we assume an extreme case that an isolated MSWI FA of 110 cm diameter and 100 cm depth in a container is exposed to the atmosphere. The bag is made of either coated air-tight sheet or uncoated standard Flecon sheet of the air permeability of 3.5 cm^3/cm^2·s, and the top of the container is opened to the atmosphere. Since all the parameters for the calculation of the time of Cs leaking are given in Table 5, the time of the leaking from MSWI FA with volume V

is now reduced to find the condition of

$$W_T = w_{max}V \quad \cdots\cdots\cdots\cdots\cdots\cdots\cdots\cdots\cdots \quad (22)$$

by numerically solving Eqs. (15) and (19). As shown in Table 5, the minimum time for Cs leaking is estimated to be 11 years for FA1 in a container composed of a standard air-permeable Flecon sheet. Since the minimum time is obtained under a severe condition that MSWI FA in an air-permeable container is stored in isolation under open atmosphere, the actual minimum time may be much longer than 11 years. However, since more than 6 years has been passed after the accident, periodic inspection of the stored MSWI FA is necessary for the safe storage.

4. Conclusion

It was found that radioactive Cs is possible to be leaked out of stored MSWI FA by absorbing moisture from the atmosphere. The mechanism of moisture absorption is repeated water absorption-evaporation cycles and capillary suction from the surface to the interior of the FA. The leaking starts when all the pores in MSWI FA are filled with a solution generated by the moisture absorption of $CaCl_2$, NaCl and KCl in the FA. 1 cm^3 of insoluble solids in the FA can support about 1.7 cm^3 of the solution without leaking. The time period for the leaking can be calculated with simple diffusion equations irrespective of the complexity of the absorption mechanism. Parameters necessary for the calculation are the initial content of water, weight-averaged annual temperature and humidity, the content of water in equilibrium with the atmosphere at the annual temperature and humidity, and the pseudo diffusion coefficient for moisture absorption. Their values can be determined by simple experiments.

Fig. 20   Rate constants of moisture absorption for MSWI FA stored in Fukushima prefecture

References

1)   S. Mizokami ,Y. Kumagai: Chapter 2. Event Sequence of the Fukushima Daiichi Accident. In "Reflections on the Fukushima Daiichi Nuclear Accident .Toward
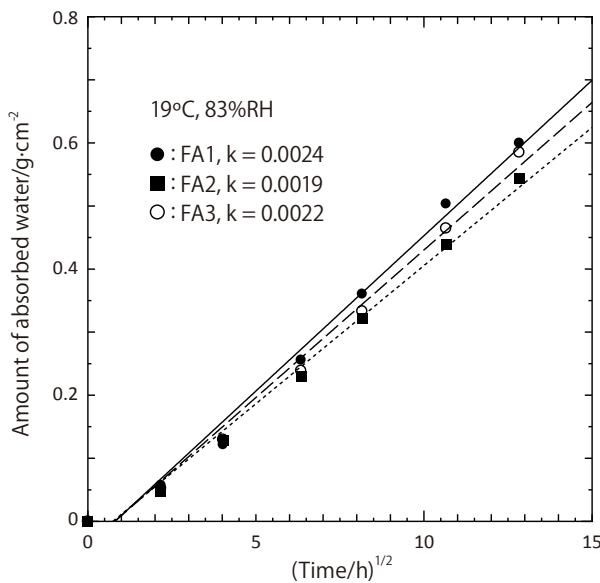
Social-Scientific Literacy and Engineering Resilience", Eds. by J. Ahn, C. Carson, M. Jensen, K. Juraku, S. Nagasaki, S. Tanaka, Springer Open, pp.21-50 (2015).

2) Y. Morino, T. Ohara, M. Nishizawa: Atmospheric behavior, deposition, and budget of radioactive materials from the Fukushima Daiichi nuclear power plant in March 2011. *Geophys. Res. Lett.*, **38**, L00G11 (2011).

3) Y. Morino, T. Ohara, M. Watanabe, S. Hayashi, M. Nishizawa: Episode Analysis of Deposition of Radiocesium from the Fukushima Daiichi Nuclear Power Plant Accident. *Environ. Sci. Technol.*, **47**, 2314-2322 (2013).

4) S. Tanaka, S. Kado: Chapter 3. Analysis of Radioactive Release from the Fukushima Daiichi Nuclear Power Station. In "Reflections on the Fukushima Daiichi Nuclear Accident .Toward Social-Scientific Literacy and Engineering Resilience" Eds. by J. Ahn, C. Carson, M. Jensen, K. Juraku, S. Nagasaki, S. Tanaka, Springer Open, pp.51-84 (2015).

5) Ministry of the Environment, Japan, Management of off-site Waste Contaminated with Radioactive Materials due to the Accident at Fukushima Nuclear Power Stations, http://www.env.go.jp/en/focus/docs/files/20121128-58.pdf, Nov. 28 (2012).

6) S. Nagasaki: Chapter 15. Radioactive Waste Management After Fukushima Daiichi Accident. In "Reflections on the Fukushima Daiichi Nuclear Accident .Toward Social-Scientific Literacy and Engineering Resilience" Eds. by J. Ahn, C. Carson, M. Jensen, K. Juraku, S. Nagasaki, S. Tanaka, Springer Open, pp.297-308 (2015).

7) Center for Material Cycles and Waste Management Research (National Institute for Environmental Studies), Proper treatment of wastes contaminated by radioactive substances, http://www.nies.go.jp/shinsai/techrepo_publicver_e_121128.pdf, Nov. 28 (2012).

8) D. Parajuli, H. Tanaka, Y. Hakuta, K. Minami, S. Fukuda, K. Umeoka, R. Kamimura, Y. Hayashi, M. Ouchi, T. Kawamoto: Dealing with the Aftermath of Fukushima Daiichi Nuclear Accident: Decontamination

of Radioactive Cesium Enriched Ash. *Environ. Sci. Technol.*, **47**, 3800–3806 (2013).

9) H. Kuramochi, M. Osako: Behavior of radioactive cesium during incineration of municipal wastes contaminated by radioactive fallout from the Fukushima Nuclear Accident. 4th EuCheMS Chemistry Congress, *Chem. Listy*, **106(S)**, s636 (2012).

10) Center for Material Cycles and Waste Management Research (National Institute for Environmental Studies), Behavior of radioactive cesium in leachate treatment facility of final waste disposal site, http://www.env.go.jp/jishin/attach/haikihyouka_kentokai/07-mat_3.pdf, p-3 (2012).

11) J. Partanen, P. Backman, R. Backman1, M. Hupa: Absorption of HCl by limestone in hot flue gases. Part II: importance of calcium hydroxychloride. *Fuel*, **84**,1674–1684 (2005).

12) F. Bodénan, Ph. Deniard: Characterization of flue gas cleaning residues from European solid waste incinerators: assessment of various Ca-based sorbent processes. *Chemosphere*, **51**, 335–347 (2003).

13) R. Yan, T. Chin, D.T. Liang, K. Laursen, W.Y. Ong, K. Yao, J.H. Tay: Kinetic Study of Hydrated Lime Reaction with HCl. *Environ. Sci. Technol.*, **37**, 2556-2562 (2003).

14) K. Kasuya, N. Onodera, A. Iizuka, E. Shibata, T. Nakamura: Reaction of Tricalcium Aluminate with Hydrogen Chloride under Simulated Bag Filter Conditions. *Ind. Eng. Chem. Res.*, **51**, 6987−6990 (2012).

15) R.H. Stokes, R.A. Robinson: Standard Solutions for Humidity Control at 25ºC. *Ind. Eng. Chem.*, **41**, 2013(1949).

16) The Chemical Society of Japan: "Kagaku Binran" (Handbook of Chemistry), 5th ed., Vol. 2, Maruzen, Tokyo, pp. II-291, (2003) [in Japanese].

17) The Chemical Society of Japan: "Kagaku Binran" (Handbook of Chemistry), 5th ed., Vol. 2, Maruzen, Tokyo, pp. II-8, (2003) [in Japanese].

18) Japan Meteorological Agency, Annual Climate of Onahama 2013, http://www.data.jma.go.jp/obd/stats/etrn/index.php (2015)